NODE SELECTION FOR UNATTENDED GROUND SENSOR NETWORKS WHILE INTERROGATING MULTIPLE TARGETS*

Qiang Le[1,2] Lance M. Kaplan[1] James H. McClellan[2]

[1]CTSPS
Dept. of Engineering
Clark Atlanta University
Atlanta, GA 30314

[2]CSIP
School of ECE
Georgia Institute of Technology
Atlanta, GA 30332-0250

ABSTRACT

This work investigates the performance of a multiple target tracker that exploits bearings-only measurements from a network of unattended ground sensors (UGS). To conserve energy while interrogating multiple maneuvering targets, the tracker integrates node resource management with the multiple-mode probabilistic data association (PDA) or joint probabilistic data association(JPDA) filter. Experiments show that for sufficiently separated targets, the global node selection leads to better geolocation performance than the 'closest' selection approach when the number of active nodes is set to two per snapshot. A track purity metric is also calculated to quantify the quality of the measurement-to-track association performance of the tracking filter.

1 INTRODUCTION

Dense networks of unattended ground sensors (UGS) promise to provide an effective and affordable solution for surveillance and reconnaissance. Such networks can be used for perimeter (or flank) protection. It is envisioned that each node on the network, i.e., the individual UGS, will communicate with each other in order to self-organize into an effective system to detect, identify and localize threats. To enhance the sustainability and survivability of the soldier, it is important that the UGS network be able to effectively collect and fuse information for as long as possible. To this end, it is very important to develop resource management techniques so that only the most effective UGS nodes are collecting, sharing and disseminating information to the solider.

This work presents our current progress to develop the resource manager that will integrate into the decentralized data fusion architecture being developed under the ARL Advanced Sensors CTA (Filipov et al. 2004). In prior work, we developed automated methods to select active nodes for tracking a single target when the nodes consist of microphone arrays that estimate the direction of arrival (DOA) of ground vehicles (Kaplan et al. 2002; Kaplan 2003; Le et al. 2004). In this work, we integrate the global node selection approach with more sophisticated filtering methods to track multiple targets. Specifically, we evaluate multiple-mode (MM) probabilistic data association (PDA) and MM joint probabilistic data association (JPDA) (Bar-Shalom and Li 1995) filters using node selection over real data collected by the U.S Army Research Laboratory (ARL).

*Prepared through collaborative participation in the Advanced Sensors Collaborative Technology Alliance sponsored by the U.S. Army Research Laboratory under Cooperative Agreement DAAD19-01-2-008.

2 MEASUREMENT AND DYNAMICAL MODEL

In this paper, the position and velocity for the t-th target are labeled as $P^t = [P_x^t, P_y^t]^T$ and $V^t = [V_x^t, V_y^t]^T$, respectively. The state for the t-th target $x^t(k)$ at time k is concatenated by the target position and velocity, i.e. $x^t(k) = [P^{tT}, V^{tT}]^T$. The bearing angles are used as the measurements. The UGS network consists of N_s nodes where the $j-th$ node reports m_j measurements at a given snapshot. The l-th measurement reported by the j-th node at snapshot time k is related to the target state via the nonlinear equation

$$z_j^l(k) = H_j(x^{f(l)}(k)) + \eta_j^l(k)$$

where

$$H_j(x^t) = \arctan\left(\frac{P_y^t - S_{j,y}}{P_x^t - S_{j,x}}\right) \quad (1)$$

is the bearing angle and $S_j = [S_{j,x}S_{j,y}]$ is the position of the the j-th node. The state index $f(l)$ represents the measurement-to-target (or track) association. The measurement error $\eta_j^l(k)$ is modeled as zero mean Gaussian noise with variance σ^2. This error is uncorrelated between the different measurements and nodes, i.e., $E\{\eta_i^p(k)\eta_j^l(k)\} = \sigma^2\delta_{i,j}\delta_{l,p}$.

Report Documentation Page

Form Approved
OMB No. 0704-0188

1. REPORT DATE	2. REPORT TYPE	3. DATES COVERED
00 DEC 2004	**N/A**	**-**

4. TITLE AND SUBTITLE	5a. CONTRACT NUMBER
Node Selection For Unattended Ground Sensor Networks While Interrogating Multiple Targets	5b. GRANT NUMBER
	5c. PROGRAM ELEMENT NUMBER
6. AUTHOR(S)	5d. PROJECT NUMBER
	5e. TASK NUMBER
	5f. WORK UNIT NUMBER
7. PERFORMING ORGANIZATION NAME(S) AND ADDRESS(ES) **Dept. of Engineering School of ECE Clark Atlanta University Atlanta, GA 30314; School of ECE Georgia Institute of Technology Atlanta, GA 30332-0250**	8. PERFORMING ORGANIZATION REPORT NUMBER
9. SPONSORING/MONITORING AGENCY NAME(S) AND ADDRESS(ES)	10. SPONSOR/MONITOR'S ACRONYM(S)
	11. SPONSOR/MONITOR'S REPORT NUMBER(S)

12. DISTRIBUTION/AVAILABILITY STATEMENT
Approved for public release, distribution unlimited

13. SUPPLEMENTARY NOTES
See also ADM001736, Proceedings for the Army Science Conference (24th) Held on 29 November - 2 December 2004 in Orlando, Florida., The original document contains color images.

14. ABSTRACT

15. SUBJECT TERMS

16. SECURITY CLASSIFICATION OF:			17. LIMITATION OF ABSTRACT	18. NUMBER OF PAGES	19a. NAME OF RESPONSIBLE PERSON
a. REPORT **unclassified**	b. ABSTRACT **unclassified**	c. THIS PAGE **unclassified**	**UU**	**8**	

The target motion can be represented by the coordinated turn (CT) dynamic model where the mode parameter is denoted by the turn rate ω,

$$x(k+1) = F(\omega)x(k) + Av(k+1), \tag{2}$$

where

$$F(\omega) = \begin{bmatrix} 1 & 0 & \frac{\sin\omega T}{\omega} & \frac{\cos\omega T - 1}{\omega} \\ 0 & 1 & \frac{1-\cos\omega T}{\omega} & \frac{\sin\omega T}{\omega} \\ 0 & 0 & \cos\omega T & -\sin\omega T \\ 0 & 0 & \sin\omega T & \cos\omega T \end{bmatrix},$$

and

$$A = \begin{bmatrix} 0.5T^2 & 0 \\ 0 & 0.5T^2 \\ T & 0 \\ 0 & T \end{bmatrix}.$$

The vector $v(k+1)$ is the process noise assumed to be Gaussian with covariance $\sigma_\mu^2 I$. We also need a stationary dynamical model to follow a stationary or low-velocity target, i.e., the dynamic matrix

$$F = \begin{bmatrix} 1 & 0 & 0 & 0 \\ 0 & 1 & 0 & 0 \\ 0 & 0 & 0 & 0 \\ 0 & 0 & 0 & 0 \end{bmatrix}.$$

3 THE TRACKER

The measurement equation and the set of dynamical models leads to a bank of extended Kalman filters (EKF). This section discusses how the tracker integrates the Kalman filtering and node selection. Based upon empirical evidence, the tracker sets the bearing error $\sigma = 5^\circ$ for this work. The subsequent sections provide experimental results for the process noise parameter σ_μ^2 that leads to the smallest root mean squared (RMS) position error.

The integration of the node selection and filtering in the tracker is illustrated in Figure 1. The initialization methods are described in the following subsection. The subsequent subsections describe the modules in Figure 1. At this point, the track manager simply maintains the current tracks over the entire data collection interval. In future work, we will develop a track manager to initiate new tracks and kill old ones.

3.1 Initialization

Multiple tracks are initialized (see (Kaplan et al. 2001)) by minimizing

$$C(P) = \sum_{j=1}^{N_s} \min_l |z_j^l(k) - \angle(P - S_j)|^2. \tag{3}$$

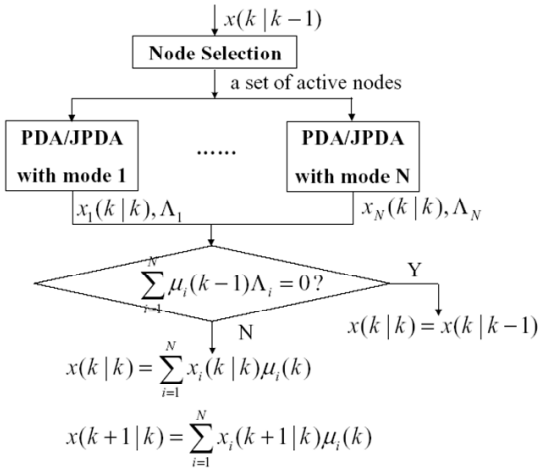

Figure 1: Structure of node selection with MM-PDA or MM-JPDA.

The number of bearing measurements m_j varies at different nodes because of false alarms and missed detection. Some of the local minima should correspond to true targets. However, other local minima could appear due to ghosting and noise. For this work, the location of the local minima closest to the ground truth target positions are used to initialize the Kalman filters. Furthermore, the initial velocity is set to zero. We also considered another initialization using the true target positions. Future work will use all local minima to initialize tracks. Then, the track manager can kill false tracks.

3.2 Probabilistic Data Association (PDA) and Joint PDA (JPDA)

In PDA/JPDA, the number of estimated tracks is assumed or maintained by the track manager. In the filtering stage, each track is updated using a weighted sum of measurement residuals via

$$x(k|k) = x(k|k-1) + \sum_{j=1}^{N_s} W_j \sum_{l=1}^{\tilde{m}_j} \beta_j^l (z_j^l(k) - z_j(k|k-1)), \tag{4}$$

$$P^{-1}(k|k) = P^{-1}(k|k-1) + P_d P_g \sum_{j=1}^{N_s} \frac{1}{\sigma_j^2} \nabla H_j \nabla H_j^T, \tag{5}$$

where P_d and P_g represent the probability of detecting a measurement and the probability the measurement passes the gating threshold, respectively. $\tilde{m}_j$ is the number of the validated measurements defined by P_g. Furthermore, W_j is the Kalman gain and ∇H_j is the Jacobian of H_j as given in (1), i.e.,

$$\nabla H_j \nabla H_j^T = \frac{1}{r_j} \begin{bmatrix} \sin\phi_j & \cos\phi_j \end{bmatrix},$$

where r_i and ϕ_i are the 2-D polar coordinates for the position of the ith node relative to the target. Finally, β_j^l is the association probability, i.e., the likelihood that the l-th measurement should be associated to a given track.

Both PDA and JPDA use a gate to eliminate measurement-to-track associations that are clearly poor. Simply given a an existing target track t, $\epsilon = \frac{(z_j(k)-z_j^t(k|k-1))^2}{\tilde{\sigma}_j^2}$ follows a chi-squared distribution with 1-degree of freedom. Note that $\tilde{\sigma}_j = \nabla H_j P_i(k|k-1) \nabla {H_j}^T + \sigma_j^2$, where $z_j(k|k-1)$ and $P(k|k-1)$ are the predicted measurement and covariance, respectively. The gate probability P_g =Pro($\epsilon < g^2$) is a user defined parameter. Once it is set, g can be computed. Then, the validated measurements of node j for track t are $\{z_j^l(k) | \frac{|z_j^l(k)-z_{ij}^t(k|k-1)|}{\tilde{\sigma}_j} < g, l = 1, 2, \ldots, m_j\}$. Clearly, the size of the validated measurement set is $\tilde{m}_j$ for a given track.

In PDA, one of the validated measurements is originated from an existing target, and the remainder are of random clutter, which does not take into account that one out of the remaining measurements may come from anther target. We assume the detection probability is the same for each node and each target. Assuming a uniform clutter distribution, the probability that none of the measurements are target originated is

$$\beta_j^0 = \frac{b}{b + \sum_{l=1}^{l=\tilde{m}_j} \wedge_j^l}, \tag{6}$$

and the probability that measurement l is target originated is

$$\beta_j^l = \frac{\wedge_j^l}{b + \sum_{l=1}^{l=\tilde{m}_j} \wedge_j^l}, \tag{7}$$

where $\wedge_j^l$ is the likelihood that $z_j^l(k)$, i.e., the l-th validated measurement from node j, is associated to the track so that

$$\wedge_j^l = \mathcal{N}(z_j^l(k); z_j(k|k-1), \tilde{\sigma}_j^2). \tag{8}$$

In other words, if the measurement is actually associated to the track, then the measurement residual is zero mean Gaussian with variance $\tilde{\sigma}_j^2$. Also, $b = \frac{\tilde{m}_j}{V}(1 - P_d P_g)/P_d$ where V is the volume of the gate. Explicitly, $V = 2g|\tilde{\sigma}_j|^{0.5}$.

The JPDA tracker is similar to the PDA tracker with the exception of the calculation of the target/measurement association probability (Bar-Shalom and Li 1995; Roecker 1994). Since the JPDA takes into account the existence of the multiple targets, the target/ measurement association probability must be marginal, i.e., the probability of track t being associated with measurement l for node j is computed by enumerating all possible joint events that contains association (t, l). Therefore, $\beta_j^l = \sum P\{\theta\}/c$ where θ is a joint event that contains an association (t, l) and c is a normalization constant. A joint event is a set of measurement-to-track associations which have measurements assigned to either clutter or tracks and each track assigned to only one measurement or declared missed. The probability of any joint event is computed by

$$\begin{aligned} P\{\theta\} &= \frac{\phi!}{V^\phi} \prod_{l=1}^{m_j} \{\mathcal{N}(z_j^l; z_j^t(k|k-1), \tilde{\sigma}_{j,t}^2)\}^{\tau_l} \\ &\quad \times \prod_{t=1}^{N_t} (P_d)^{\delta_t} (1 - P_d)^{\delta_t}, \end{aligned}$$

where ϕ is the number of clutter hits, τ_l is a binary number indicating whether measurement l is assigned to a track t, δ_t is a binary number indicating whether on not track t is assigned to a measurement, and N_t is the number of tracks. Given a case with a total of four measurements, where Measurements 1 and 4 both fall inside the gates of the two established tracks, but Measurement 2 can only be associated with Track 1 and Measurement 3 can only be associated with Track 2, then there are four joint events that contains the association of Track 1 with Measurement 2 (1,2):

- $\theta_1 = (1, 2), (2, 1)$, (clutter, 3&4),
- $\theta_2 = (1, 2), (2, 3)$, (clutter, 1&4),
- $\theta_3 = (1, 2), (2, 4)$, (clutter, 1&3),
- $\theta_4 = (1, 2), (2,$ missed),(clutter,1&3&4).

3.3 Multiple-mode(MM) Tracking

The MM tracker (Bar-Shalom and Li 1995) employs a bank of mode-matched filters that can represent a standard EKF, a PDA filter or a JPDA filter (see Figure 1). The initial state and covariance for each mode-matched filter is the same and given by the previous global state and covariance in the MM. The global state update is the weighted sum of the state outputs of each mode-matched filter expressed by

$$x(k|k) = \sum_{i=1}^{N} x_i(k|k)\mu_i(k), \tag{9}$$

where $\mu_i(k)$ is the mode probability, $x_i(k|k)$ is the state output of the ith mode-matched filter and N is the number of the mode-matched filters. Likewise, the covariance update is given by

$$\begin{aligned} P(k|k) &= \sum_{i=1}^{N} \{(x(k|k) - x_i(k|k))(x(k|k) - x_i(k|k))^T \\ &\quad + P_i(k|k)\}\mu_i(k), \end{aligned}$$

where $P_i(k|k)$ is the covariance output of the i-th mode-matched filter.

The weights $\mu_i(k)$ are derived from the likelihood of each mode representing the true dynamics of the target. The measurement-to-track likelihood is computed via (8)

for each mode i and is explicitly labeled as $\wedge_{ij}^{l}$. Using the additive fusion strategy suggested in (Chen and Olson 2003), the likelihood that the target dynamics follow mode i given the current measurement set is

$$\wedge_i(k) = \sum_{j=1}^{N_s} \sum_{l=1}^{\tilde{m}_j} \wedge_{ij}^{l}. \quad (10)$$

The mode likelihood (10) measures the difference between the assumed model expressed by the predicted measurement and the true model denoted by the received measurement. In other words, if model difference is larger, the likelihood that the current measurement follows the assumed model gets smaller. Finally, the mode probability $\mu_i(k)$ is updated via Bayes rule where $\mu_(k-1)$ is the prior probability, i.e.,

$$\mu_i(k) = \frac{\wedge_i(k)\mu_i(k-1)}{\sum_{j=1}^{N} \wedge_j(k)\mu_j(k-1)}. \quad (11)$$

3.4 Node selection

A node selection algorithm is embedded in a resource manager to determine which subset of nodes will be active for a given snapshot of data collection. In this paper, we use the global node selection (GNS) approach (Kaplan 2003). The selection is global in the sense that each node knows the exact locations of all other nodes in the network. Localized node selection has also been proposed where only information about neighboring nodes is known, e.g., (Kaplan et al. 2002). A localized method will be integrated in to the multiple target tracker in future work.

GNS is a nearly optimal approach to determine which active set of nodes $\mathcal{N}_a$ provides the best geometry to localize a target. In short, the objective of the node selection is to minimize the expected RMS position error over all possible combinations of N_a nodes. Without accounting for the prior measurements, the expected RMS position error can be extracted from (5) as

$$\rho = \sqrt{\text{trace}\left\{\mathbf{J}^{-1}\right\}}, \quad (12)$$

where $\mathbf{J}$ is the Fisher information matrix (FIM), i.e., the inverse of the position covariance, such that

$$\mathbf{J} = \sum_{i \in \mathcal{N}_a} \frac{1}{\sigma_i^2} \frac{1}{r_i^2} \begin{pmatrix} \sin^2\phi_i & -\sin\phi_i\cos\phi_i \\ -\sin\phi_i\cos\phi_i & \cos^2\phi_i \end{pmatrix}. \quad (13)$$

The GNS is a Greedy simplex approach to find the best N_a nodes. It starts by determining the best two nodes via exhaustive search. Then, it adds one node at a time to the active set. Finally, single node replacements that reduce (12) are exhausted. The GNS approach reduces the computational complexity from $O(N^{N_a})$ with exhaustive search to $O(N^2)$. Effectively, the GNS method selects nodes that surround the target and are within close proximity of the target. To baseline the GNS method, we also consider the 'closest' node selection approach that selects the N_a nodes which lie closest to the predicted target location.

Figure 1 shows how node selection is integrated into the tracking filter. Prediction is critical in the combined node selection and MM-PDA/MM-JPDA due to the following reasons: 1) Node selection algorithms use the prediction to determine which subset of nodes will be active, and 2) when none of the current measurements lie in the gate for a given mode i, the mode likelihood is zero, i.e., $\wedge_i(k) = 0$. When $\sum_{i=1}^{N} \wedge_i(k)\mu_i(k-1) = 0$, we can infer that none of the assumed modes is correct. In this case, it is better to use the predicted target state and covariance instead of using the filtered ones. The predicted state and covariance in the MM-PDA/MM-JPDA with the node selection are given by (see (Blackman and Popoli 1999)):

$$x(k|k-1) = \sum_{i=1}^{N} x_i(k|k-1)u_i(k-1),$$

$$P(k|k-1) = \sum_{i=1}^{N} P_i(k|k-1)u_i(k-1),$$

where $x_i(k|k-1)$ and $P_i(k|k-1)$ are mode-related predictions.

4 TRACK METRICS

To compare trackers, we score the resulting tracks via RMS position error and track purity. These metrics are clearly defined in the following subsections.

4.1 RMS Error

The RMS position error is simply the sum of the position errors between the tracks and the corresponding target. In other words, at snapshot k, the error is

$$RMS(k) = \frac{1}{N_t} \sum_{t=1}^{N_t} \left(\sum_{s=1}^{2} ([x^t(k|k)]_s - [P^t(k)]_s)^2 \right)^{\frac{1}{2}},$$

where $[x]_s$ extracts the s-th element of vector x. The results presented in the next section report on the average RMS error over all snapshots, i.e.,

$$e = \frac{1}{N_k} \sum_{k=1}^{N_k} RMS(k).$$

4.2 Track Purity

In the experiments, we report a simple purity metric that could indicate a track switch or merge. The intent of the metric is to quantify the accuracy of a target/ measurement association algorithm in a multi-node multi-mode multi-target tracker. The correct target/ measurement association

is derived using the ground truth provided by the GPS units located in the targets. Let $C_{t,j}$ be the correct association for track t at node j. If some measurements from node j pass the gate for track t, then

$$C_{t,j} = \arg\min_{l \in \{l:|z_j^l - \theta_t| < \tau\}} |z_j^l - \theta_t|. \quad (14)$$

Otherwise, $C_{t,j} = 0$, which indicates that target t is not detected. For mode i and a chosen node $j \in \mathcal{N}_a$, the association of the target t with the measurement l is $\beta_{t,i,j}^l$ and $\sum_{l=1}^{m_j} \beta_{t,i,j}^l \leq 1$. The purity of the target/ measurement association is defined as:

$$Q_{t,i,j} = \beta_{t,i,j}^{C_{t,j}}, \quad (15)$$

if $C_{t,j} \neq 0$. Otherwise if $C_{t,j} = 0$,

$$Q_{t,i,j} = 1 - \sum_{l=1}^{m_j} \beta_{t,i,j}^l.$$

Considering, all active nodes, the average purity is

$$Q_{t,i} = \frac{1}{N_a} \sum_{j \in \mathcal{N}_a} Q_{t,i,j}.$$

The average purity of the target/measurement association is

$$Q_t = \sum_{i=1}^{N} \mu_i(k) Q_{t,i}, \quad (16)$$

where $\mu_i(k)$ is computed in (11). Finally, the purity of the measurement-to-target associations Q_m is the average value of Q_t over the number of the targets.

5 Experiments

The real data, collected by the U.S. Army Research Laboratory (ARL) at Aberdeen Proving Grounds, contains multiple targets traveling along an oval track or an adjacent road. Six acoustic nodes were situated in the middle of the track. The targets were fitted with GPS to obtain ground truth information. Figure 2 shows the tracks of targets for two different test scenarios and the initial position estimates as computed by the method in Section 3.1.

ARL processed the raw data using an incoherent wideband minimum variance distortionless response (MVDR) beamformer (Wilson et al. 2002) to obtain bearing measurements. Figures 3 and 4 show the bearing measurements obtained by different nodes for different test scenarios. In Scenario 1, one target is traveling along the track, while the other target is traveling down the road parallel to the track. In Scenario 2, a convoy of four vehicles is traveling around the track. The measurements are assumed to have 5° errors for each snapshot. However, at each node, the bearing measurements can be missed and false measurements could be detected. Clearly, in Figure 4, two measurement tracks are

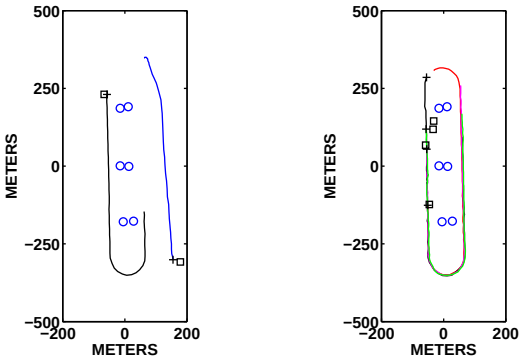

Figure 2: Node locations and tracks: (a) Scenario 1, and (b) Scenario 2. The circles represent the node locations, the plus symbols represent the initial target positions, the square symbols represent the estimated target positions, and the lines represent the target trajectories.

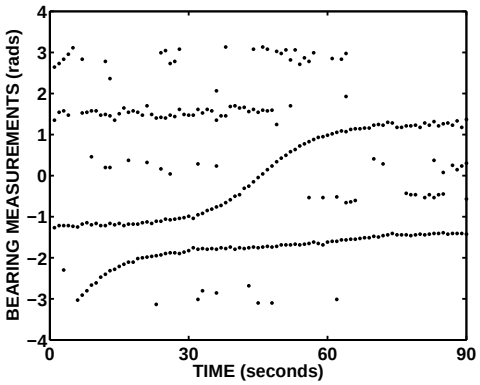

Figure 3: Bearing measurement output of MVDR for the top right node in Scenario 1.

obvious for k between 40 to 130. However, a large number of false measurement are also obtained. On the other hand, three measurement tracks exist for k between 130 to 200. However, in these snapshots, the targets are not always detected.

For both scenarios, we initialize two tracks. In Scenario 1 the number of targets is correctly modeled, but for Scenario 2, it is underestimated. The purpose for underestimating the number of targets in Scenario 2 is to avoid the occurrence of track swaps or mergence, which leads to poor geolocation performance. For Scenario 2, we either track the front and back targets, or the two middle targets. Clearly, the middle targets pose a greater challenge to the measurement-to-track association portion of the track filter.

In these experiments, P_d and P_g are fixed to be 0.9999 for Scenario 1, and 0.98 for Scenario 2. Here, we do not consider adaptive setting of P_d or P_g. A bank of four mode-matched filters are used where 3 modes represent the CT

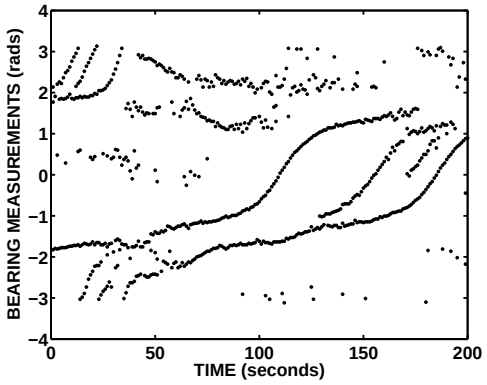

Figure 4: Bearing measurement output of MVDR for the middle left node in Scenario 2.

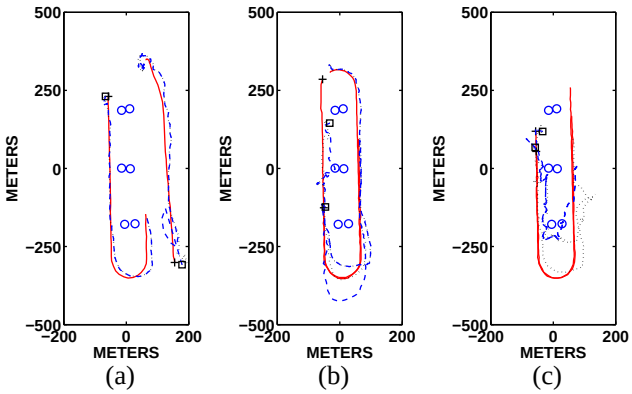

Figure 5: Estimated tracks: (a) Scenario 1, (b) Scenario 2 for the two end targets, and (c) Scenario 2 for the middle targets. In the figures, the dotted and dashed lines represent MM-JPDA and MM-PDA tracks, respectively.

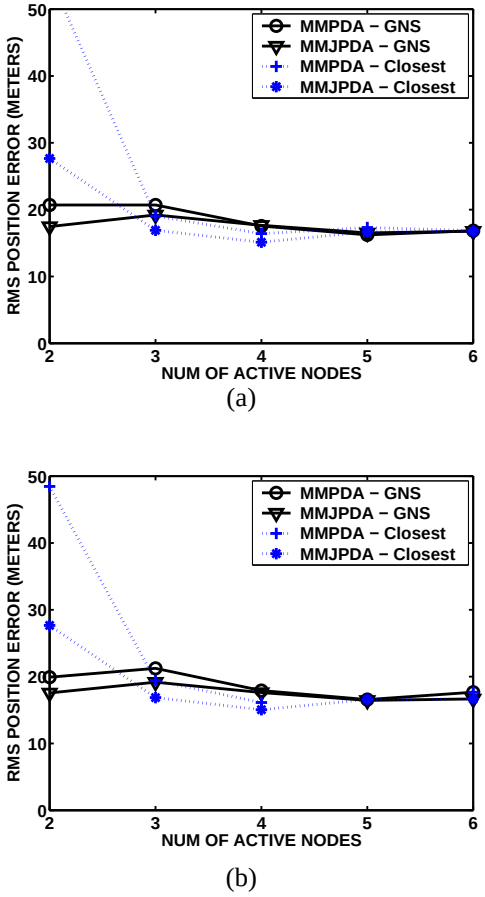

Figure 6: Average RMS errors for Scenario 1 by initialing the track filters using (a) the true target positions, or (b) estimated target positions via (3).

model for $\omega \in \{-20^\circ, 0^\circ, 20^\circ\}$, and the final mode represents a stationary dynamical model. The initial mode probability $\mu_i(0)$ is set uniformly so that $\mu_i(0) = 1/4$.

Figure 5 shows the estimated tracks using MM-PDA or MM-JPDA when all nodes are active and the process noise parameter σ_ν is set to a value that minimized the RMS position error. We considered different values for σ_ν between 1 m^2/s to 21 m^2/s in intervals of 2 m^2/s. The target states were initialized via (3). The figure shows that the MM-PDA method has the most severe adaptation delay around the corner while the MM-JPDA has the slightest adaptation delay.

Next, we evaluated the multiple target trackers using the GNS method for different values of N_a. We also considered a simplified node selection method that selects the closest N_a nodes to the predicted target positions. Figures 6-8 show the average RMS position errors for the different approaches using either (3) or the true target positions for initialization. Again, the best process noise is used. For Scenario 1, it is clear in Figure 6 that the MM-JPDA is more effective than the MM-PDA and GNS outperforms the 'closest' selection approach when $N_a = 2$ for different initializations of the filters.

For Scenario 2, we intend to track the top and bottom targets, or the middle two targets along the oval tracks. Figure 7 shows that when tracking the end targets, GNS is able to maintain localization performance as N_a goes to two. MM-JPDA with GNS is robust even when the initial guesses are noisy. However, other combination of track filters and node selection is poor at some value of N_a. Figure 8 shows that when tracking the middle two targets in Scenario 2, the average RMS errors are almost always more than 70 meters. Note that the average distances between two adjacent targets from top to bottom are 107, 77 and 201 meters, respectively. Inspection of the tracks actually indicate that track mergence and swaps occur during the lifetime of the tracks while attempting to follow the middle targets.

Table 1 and 2 quantify the RMS and track purity performance of MM-PDA/ MM-JPDA with different nodes selection methods when $N_a = 2$. Usually, a higher purity score

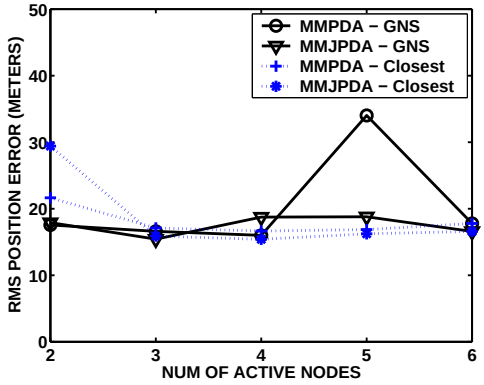

(a)

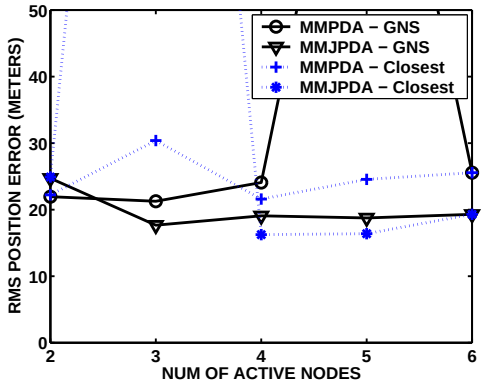

(b)

Figure 7: Average RMS errors for Scenario 2 to track top and bottom targets by initialing the track filters using (a) the true target positions, or (b) estimated target positions via (3).

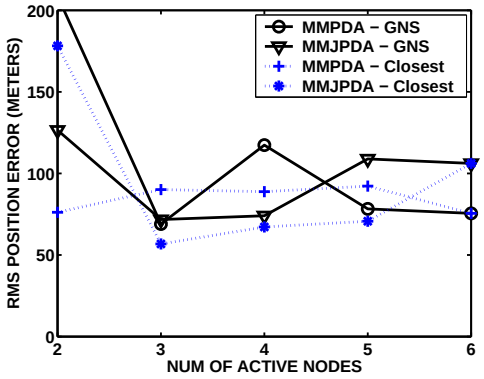

(a)

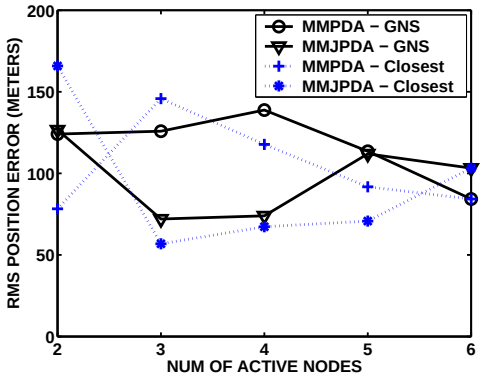

(b)

Figure 8: Average RMS errors for Scenario 2 to track middle two targets by initialing the track filters using (a) the true target positions, or (b) estimated target positions via (3).

	Scenario 1			
	PDA GNS	JPDA GNS	PDA closest	JPDA closest
RMS err.(m)	20.69	17.46	54.93	27.65
Q_m	0.970	0.981	0.966	0.969
	Scenario 2 to track top and bottom targets			
	PDA GNS	JPDA GNS	PDA closest	JPDA closest
RMS err.(m)	17.55	17.91	21.63	29.41
Q_m	0.935	0.932	0.929	0.886
	Scenario 2 to track middle two targets			
	PDA GNS	JPDA GNS	PDA closest	JPDA closest
RMS err.(m)	208.8	126.5	76.19	178.1
Q_m	0.277	0.242	0.429	0.264

Table 1: Track purity and corresponding average RMS positions errors with $N_a = 2$ when initialing the filters using true target positions.

	Scenario 1			
	PDA GNS	JPDA GNS	PDA closest	JPDA closest
RMS err.(m)	19.90	17.55	48.45	27.66
Q_m	0.968	0.981	0.944	0.967
	Scenario 2 to track top and bottom targets			
	PDA GNS	JPDA GNS	PDA closest	JPDA closest
RMS err.(m)	21.95	24.71	22.21	24.90
Q_m	0.905	0.890	0.923	0.903
	Scenario 2 to track middle two targets			
	PDA GNS	JPDA GNS	PDA closest	JPDA closest
RMS err.(m)	124.0	126.6	78.28	165.8
Q_m	0.359	0.243	0.427	0.090

Table 2: Track purity and corresponding average RMS positions errors with $N_a = 2$ when initialing the filters via (3).

translates to a lower RMS positions error. It is noted that a high purity score with large RMS errors is possible because the collection geometry can be poor. For example, in Scenario 1 the MM-PDA using the 'closest' method lead to the worst estimation performance, but the purity Q_m is above 0.9. The MM-JPDA using GNS has the smallest RMS errors and highest Q_m no mater how the filters are initialized. In Scenario 2, when tracking the top and bottom targets, the purity Q_m is at least 0.8. When tracking the middle two targets, the purity, Q_m is poor and below 0.5. The poor purity explains the poor RMS error values.

6 Conclusions

This paper evaluates the utility of node selection integrated into a multiple-mode data association tracking filter. Experiments on real data show that the MM-JPDA filters are more effective than MM-PDA filters. When implementing node selection, GNS demonstrates an obvious advantage over the 'closest' node selection when the number of active nodes per snapshot is set to two. However, for the trackers to be effective, the targets being tracked must be sufficiently separated. When targets are close, tracks can either merge or swap. Apparently, a target separation in the order of 70 meters is not sufficient for tracking.

Future work will investigate the performance of the trackers when using a more sophisticated track manager. We also plan to determine the limits of the MM-PDA and MM-JPDA when using node selection for closely separated targets. We also plan to investigate the utility of a multiple hypothesis tracker (MHT) for closely spaced targets Blackman and Popoli (1999). Finally, we plan to integrate localized node selection into the tracker.

References

Bar-Shalom, Y. and X.-R. Li: 1995, *Multitarget-Multisensor Tracking: Principles and Techniques*. YBS.

Blackman, S. and R. Popoli: 1999, *Design and Analysis of Modern Tracking Systems*. Artech House, Boston.

Chen, H.-W. and T. Olson: 2003, Adaptive spatiotemporal multiple sensor fusion. *Optical Engineering*, **42**, 1481–1495.

Filipov, A., N. Srour, and M. Falco: 2004, Distributed and disposable sensors at ARL and the ASCTA. *Proc. of IEEE Aerospace Conference*, Big Sky, MT.

Kaplan, L. M.: 2003, Node selection for target tracking using bearing measurements from unattended ground sensors. *Proc. of the IEEE Aerospace Conference*, Big Sky, MT, volume 5, 2137–2152.

Kaplan, L. M., P. Molnar, and Q. Le: 2001, Bearings-only target localization for an acoustical unattended ground sensor network. *Proc. of SPIE*, volume 4393, 40–51.

Kaplan, L. M., P. Molnar, N. Srour, and A. Filipov: 2002, Autonomous node selection for wireless networks of bearings-only sensors. *Proc. of the 23rd Army Science Conference*, Orlando, FL.

Le, Q., Jim.McClellan, and L. M. Kalan: 2004, Multiple-mode Kalman filtering with node selection using bearings-only measurements. *36th IEEE Southeastern Symposium on SystemTheory (SSST)*, volume 36, 185–189.

Roecker, J.: 1994, A class of near optimal JPDA algorithms. *IEEE Trans. on Aerospace and Electronic Systems*, **30**, 504–510.

Wilson, D. K., B. M. Sandler, and T. Pham: 2002, Simulation of detection and beamforming with acousitcal ground sensors. *Proc. of SPIE*, volume 4743, 50–61.

The views and conclusions contained in this document are those of the authors and should not be interpreted as presenting the official policies either express or implied of the Army Research Laboratory or the U. S. Government.